Intermolecular Spectrum of Liquid Biphenyl Studied by Optical Kerr Effect Spectroscopy

Justin Rajesh Rajian, Byung-Ryool Hyun,† and Edward L. Quitevis*

Department of Chemistry and Biochemistry and Department of Physics, Texas Tech University, Lubbock, Texas 79409

Received: June 15, 2004; In Final Form: August 24, 2004

The intermolecular spectra of neat liquid biphenyl and biphenyl/*n*-heptane mixtures were obtained by using optically heterodyne detected optical Kerr effect (OHD-OKE) spectroscopy. The intermolecular spectrum of biphenyl is broad and bimodal in character. The spectrum of biphenyl undergoes a red shift and line narrowing with temperature and upon dilution in *n*-heptane. The spectra can be well fit by a bimodal line shape function. Inconsistencies, however, arise in the interpretation of the effects of temperature and dilution on the individual component bands. The spectrum of biphenyl is similar in frequency and width to that of benzene. Packing models suggest that rotational motion is more hindered in biphenyl than in benzene, which could explain the similarity of the spectra of the two liquids, even though the moments of inertia for the two molecules are quite different.

I. Introduction

Within the past decade, experiments devoted to obtaining the low-frequency (0−250 cm^{-1}) spectra of liquids by optical Kerr effect (OKE) spectroscopy have flourished.[1−3] The aim of these experiments is to understand the intermolecular dynamics in these systems. For liquids composed of simple linear molecules, such as CS_2, the spectra are smooth and featureless. For these liquids, the liaison of experiment with molecular dynamics (MD) simulations has led to a detailed understanding of the molecular motions that underlie the spectra.[4,5] For more complex molecules, MD simulations, however, are sparse compared to the number of experiments.[6−8] Phenomenological approaches, because of their ease of implementation, have provided experimentalists with a way of interpreting the spectra of these systems. These approaches work reasonably well for certain liquids. For example, McMorrow et al.,[9] using an inhomogeneously broadened quantum harmonic oscillator (HO) model, were able to explain the evolution of the spectrum of CS_2 on dilution in weakly interacting alkane solvents. In this model, the intermolecular response is determined by the vibrational dephasing rate Γ and the characteristic frequency ω_0 and width σ of the frequency distribution. The model reproduces the shape of the intermolecular response observed experimentally and predicts the shift to lower frequency and the line narrowing of the spectrum with a minimal number of parameters. For the CS_2/alkane system, the shift to lower frequency and line narrowing that occur upon dilution can simply be accounted for by decreasing ω_0 while keeping Γ and σ constant.

The OKE spectra of certain aromatic liquids, such as benzene,[10] toluene,[1,11] benzonitrile,[11−13] hexafluorobenzene,[14] pyridine,[10] and aniline,[13] are broader and flatter than that of CS_2. The spectra are typically fit by line shape functions composed of a low-frequency component and a high-frequency component.[11,13−15] It has been suggested that the low-frequency shoulder of benzene is associated with the modes of locally ordered structures or clusters.[10] The observation that the low-frequency shoulder is reduced upon dilution in a weakly interacting solvent lends credence to this argument.[16] Chelli et al.[17,18] and Ratajska-Gadomska et al.[19,20] have taken this point of view a step further by assuming that the liquid is organized in instantaneous quasi-crystalline short-range clusters and simulating the spectrum of benzene by using the phonon modes within these clusters.

The cluster model, however, conflicts with the earlier work of Chandler and co-workers.[21,22] This work showed that the structure of a nonassociated liquid, such as benzene, is largely attributed to repulsive intermolecular forces and not to attractive forces, dipole−dipole interactions, or other slowly varying interactions. In short, intermolecular correlations are determined by molecular shape. In this regard, packing models provide an approximate picture of the local structure of a molecular liquid. For example, the arrangement of molecules in liquid benzene is not unlike the average arrangement of neighboring Cheerios in a bowl of cereal.[22]

Ryu and Stratt,[8] using MD simulations in conjunction with instantaneous normal mode (INM) analysis, were able to provide a molecular interpretation of the spectrum of benzene without invoking the existence of clusters. By incorporating projection operator techniques in the INM analysis, the extent to which specific motions influence the OKE spectrum was determined. Specifically, because of benzene's relatively low moments of inertia, the rotational component is higher in frequency than the translational component. The overall spectrum therefore appears flat and/or structured. In contrast, when the rotational and translational components are comparable in frequency and width, as in CS_2, the overall spectrum appears smooth and featureless. The characteristic shape of the OKE spectra of benzene and other aromatic liquids is attributed not to the aromaticity of the molecules, as suggested previously by other researchers,[11,12] but to the planarity of the molecules. Because planar molecules possess small moments of inertia associated with the tumbling motion, there will always be a high-frequency component in the OKE spectra of liquids composed of these types of molecules. The main conclusion from this study is that

* To whom correspondence should be addressed. E-mail: edward.quitevis@ttu.edu.

† Current address: School of Applied and Engineering Physics, Cornell University, Ithaca, NY 14853-3501.

10.1021/jp047415h CCC: $27.50
Published on Web 10/15/2004

TABLE 1: Molecular Polarizabilities[a]

molecule	α_{xx}/Å^3	α_{yy}/Å^3	α_{zz}/Å^3
benzene	12.27	12.27	6.65
biphenyl, 30° dihedral angle	24.70	20.20	13.80
n-heptane	3.28	2.78	3.41

[a] Polarizabilities were obtained from refs 23 and 52.

TABLE 2: Moments of Inertia[a]

molecule	I_A/amu	I_B/amu	I_C/amu
benzene (D_{6h})	317.385	317.385	634.770
biphenyl (D_{2h}), 0° dihedral angle	630.665	3227.849	3858.514
biphenyl (D_2), 30° dihedral angle	634.702	3256.922	3736.548

[a] RHF-AM1 calculation using Spartan V2.2 (Wavefunction, Inc.).

molecular shape and collective packing largely determine the OKE spectrum of a nonassociating liquid.

Liquid biphenyl is an interesting test case for these ideas regarding the molecular shape and the OKE spectrum of a liquid. Because of the two phenyl rings, the attractive intermolecular forces in biphenyl should be similar to those in benzene. Indeed, the elements of the molecular polarizability tensor of biphenyl are roughly twice that of benzene (Table 1).[23] The orientational dynamics, however, are very different for these two liquids because the molecules have quite different shapes and different moments of inertia (Table 2). Benzene is a symmetric ellipsoid that can rotate about the 6-fold symmetry axis perpendicular to the ring (spinning motion) and about the 2-fold axes in the plane of the ring (tumbling motion). In an OKE experiment only one relaxation time is observed corresponding to the rotation about the 2-fold axes in the plane of the ring, because there is no change in the polarizability anisotropy for rotation about the 6-fold symmetry axis. Biphenyl in the liquid phase is twisted about the central C−C bond between the phenyl rings, with a dihedral angle of 20−40°.[24,25] With respect to rotational motion, biphenyl molecules can be approximately treated as symmetric cylindrical ellipsoids. Deeg et al.[26] showed in transient grating (TG) OKE measurements on biphenyl that the diffusive part of the signal is biexponential, with a slow component, τ_s, and a fast component, τ_f, where the correlation time for rotation about the two short axes (tumbling motion) is directly given by τ_s and that for rotation about the long axis (spinning motion) is given by $\tau_x = 2\tau_f\tau_s/(3\tau_s - \tau_f)$.

In this article, we describe studies of the dynamics of liquid biphenyl by OKE spectroscopy. Since the diffusive orientational dynamics of biphenyl in the neat liquid and in *n*-heptane solution have previously been studied,[26,27] this article will focus on the intermolecular dynamics of biphenyl. This article is organized as follows. In section II, the apparatus and method of data acquisition are briefly described. In section III, the method for obtaining the reduced spectral densities is outlined. In section IV, the time-domain OKE data and reduced spectral densities are presented. The reduced spectral densities are fit to a bimodal line shape function in order to quantify the effects of temperature and dilution on the intermolecular part of the reduced spectral density. Interestingly, the reduced spectral density of biphenyl approximately overlaps the reduced spectral density of benzene, despite the differences in the moments of inertia for these two liquids. Finally, the role of molecular shape and the local structure of the liquid in possibly determining the reduced spectral densities of biphenyl and benzene is discussed.

II. Experimental Section

The 40 fs titanium−sapphire laser, OKE apparatus, and method of data acquisition have been described in detail previously.[28,29] Optical heterodyne detection (OHD) was used to linearize the signal with respect to the material response. To minimize the data collection time, scans were carried out in 10 fs steps in the −0.5 to 3 ps time range and in 100 fs steps for $t < -0.5$ ps and $t > 3$ ps. Biphenyl and *n*-heptane (Aldrich) were used without further purification. Biphenyl/*n*-heptane mixtures were prepared with biphenyl mole fractions $x_{BP} = 0.25$ and 0.50. The samples were contained in a sealed 2 mm path length UV-grade fused-silica cell (Hellma Cells). The sample cell was placed in a home-built copper cell holder with optical access and whose temperature was regulated and controlled with a thermoelectric heater/cooler system. Samples were heated to temperatures above the melting point ($T_{mp} = 341$ K) of biphenyl. Measurements were carried out on the heated samples at 348, 373, and 393 K. Because the OHD-OKE response of *n*-heptane is ∼10 times smaller than that of biphenyl, the OHD-OKE response of a binary mixture is assumed to mainly be due to biphenyl. This was also found to be true in the TG-OKE data obtained by Deeg et al.[26]

III. Analysis

The experimentally measured OHD-OKE signal is the convolution of the pulse intensity background free autocorrelation, $G_0^{(2)}(t)$, and the impulse response, $R(t)$:

$$T(\tau) = \int_{-\infty}^{\infty} G_0^{(2)}(t)\, R(\tau - t)\, \mathrm{d}t \qquad (1)$$

where $R(t)$ is given by the sum of an electronic part, which is assumed to be instantaneous on the time scale of the laser pulse, and a nuclear part. In the Fourier transform procedure,[30,31] the impulse response is represented by a frequency response function

$$D(\omega) \equiv \mathscr{F}\{R(t)\} \qquad (2)$$

where $\mathscr{F}$ denotes a forward complex Fourier transform operation. $D(\omega)$ is obtained by the complex division of the Fourier transform of the OHD-OKE signal by the Fourier transform of the pulse autocorrelation:

$$D(\omega) = \mathscr{F}\{T(\tau)\}/\mathscr{F}\{G_0^{(2)}(\tau)\} \qquad (3)$$

The imaginary part, Im $D(\omega)$, gives the spectral density of the liquid and is directly related to the depolarized Rayleigh/Raman spectrum of the liquid.[32] The diffusive part of the nuclear response, which is due mainly to orientational dynamics, is quantitatively modeled by the convolution of $G_0^{(2)}(t)$ with an empirical decay function. After "tail matching", the diffusive response function is subtracted from the OHD-OKE signal. Removal of the diffusive part of the OHD-OKE signal yields a reduced response, which contains only the electronic and nondiffusive nuclear contribution.[30] By applying the Fourier transform procedure to the reduced response, a reduced spectral density (RSD), Im $D'(\omega)$, is obtained. The RSD gives the frequency domain representation of the nondiffusive response. Within the framework of INM analysis, the intermolecular part of the RSD represents a weighted probability distribution of INM frequencies, where the weighting is given by derivatives of the anisotropic part of the many-body polarizability with respect to the INM coordinates.[4−6,8]

IV. Results and Discussion

Time-Domain Response. Figure 1 shows the temperature dependence of OHD-OKE signal as the temperature is increased

TABLE 3: Fit Parameters for the OHD-OKE Response for $t > 0.5$ ps for Neat Biphenyl, Neat *n*-Heptane, and Biphenyl/*n*-Heptane Mixtures[a]

liquid/mixture[b]	A_1	τ_1/ps	A_2	τ_2/ps	A_3	τ_3/ps
neat BP at 393 K	0.212	0.356	0.058	2.29	0.055	15.5
neat BP at 373 K	0.225	0.340	0.054	2.44	0.045	19.8
neat BP at 348 K	0.201	0.395	0.040	3.31	0.033	30.4
$x_{BP} = 0.50$ at 348 K	0.332	0.248	0.067	1.43	0.070	11.1
$x_{BP} = 0.25$ at 348 K	0.324	0.205	0.063	1.18	0.058	8.12
neat C_7 at 348 K	0.073	0.417	0.013	4.71		

[a] See eq 4 for definition of fit parameters. [b] BP, biphenyl; C_7, *n*-heptane

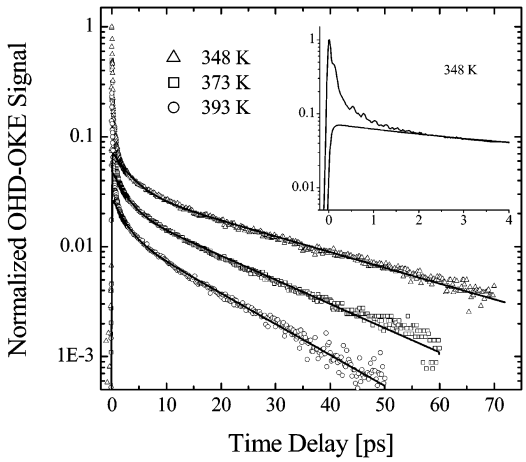

Figure 1. Semilogarithmic plot of typical OHD-OKE data for neat biphenyl at 348, 373, and 393 K. The data in this plot were normalized to the peak of the electronic response and offset for the purposes of clarity. The smooth curves are the diffusive orientational responses. The inset shows the OHD-OKE response for biphenyl at 348 K in the region between −0.2 and 4 ps.

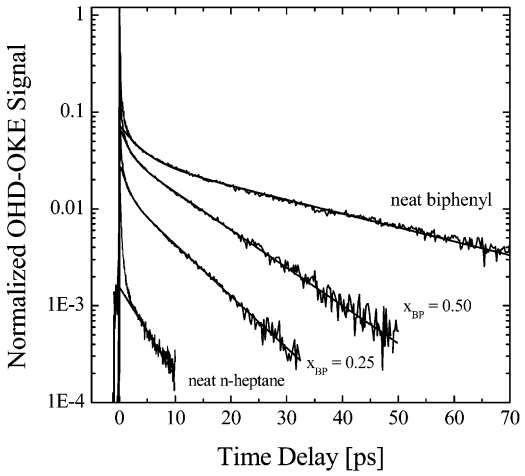

Figure 2. Semilogarithmic plots of typical OHD-OKE data at 348 K for neat biphenyl, biphenyl/*n*-heptane mixtures with $x_{BP} = 0.50$ and 0.25, and neat *n*-heptane. The data in this plot were normalized to the peak of the electronic response and offset for the purposes of clarity. The smooth curves are the diffusive orientational responses.

from 348 to 393 K. The data in these plots were normalized to the peak of the electronic response and offset for the purposes of clarity. The time range -2 ps $< t <$ 70 ps in Figure 1 spans the electronic response, the nondiffusive response, and the diffusive orientational response. The nuclear response appears as a shoulder on the electronic response that evolves into a nonexponential decay after 500 fs (Figure 1, inset). As observed previously,[26] the diffusive orientational response becomes faster with increasing temperature. To quantitatively characterize the relaxation of the OHD-OKE response, the data were fitted by a multiexponential decay function

$$r(t) = \sum_i A_i \exp(-t/\tau_i) \tag{4}$$

using nonlinear least squares. The fits were started at 0.5 ps to avoid the initial shoulder. The results of the fits are given in Table 3. The relaxation times τ_2 and τ_3, which are associated with diffusive orientational dynamics, are in good agreement with values obtained previously by Deeg et al.[26]

The characteristic initial fast decay (i.e., the shoulder on the electronic response) and pseudoexponential "tail" of the nondiffusive part of the response are evident in an enlarged view of the data between -0.5 and 4 ps (Figure 1, inset). The subpicosecond relaxation time τ_1 obtained in the fit of eq 4 to the OHD-OKE data is assumed to be the 1/e time for the pseudoexponential tail of the nondiffusive response. Superimposed on the response is an oscillatory component arising from the coherent excitation of intramolecular modes (see Spectral Densities below).

Figure 2 shows the evolution of the OHD-OKE response for biphenyl at 348 K upon dilution. The OHD-OKE response for both neat biphenyl and for the biphenyl/*n*-heptane mixtures in this time range can be well fit by three exponentials. In the case of neat *n*-heptane, the OHD-OKE response is well fit by just two exponentials. The fit parameters for the mixtures and neat *n*-heptane are given Table 3. The decrease in the values of τ_2 and τ_3 upon dilution in this time region has been observed previously by Deeg et al.[26] and in other binary systems.[9,33−36] Orientational relaxation of biphenyl should become faster as the mixture becomes richer in the less viscous *n*-heptane solvent.

Spectral Densities. We will assume that the diffusive part of the OHD-OKE response for neat biphenyl and *n*-heptane solutions of biphenyl can be quantitatively described by the convolution of the pulse intensity autocorrelation with a decay function

$$r(t) = [1 - \exp(-2t/\beta)][A_2 \exp(-t/\tau_2) + A_3 \exp(-t/\tau_3)] \tag{5}$$

with A_2, τ_2, A_3, and τ_3 being the values obtained from the nonlinear least-squares fits of eq 4 to the data. In the case of neat *n*-heptane, only a single exponential with a relaxation time equal to τ_2 was used. The $\beta/2$ rise time takes into account the fact that nuclear responses cannot follow the intensity profile of short pulses. In this study, β was set equal to $1/\langle\omega\rangle$, where $\langle\omega\rangle$ is the first moment of the spectral density. The smooth curves in Figures 1 and 2 are the tail-matched diffusive responses.

Figure 3 depicts the full spectral densities at 348 K over the frequency range 0−425 cm^{-1} for neat biphenyl, biphenyl/*n*-heptane mixtures, and neat *n*-heptane. There are six vibrational modes associated with the relative motion of the phenyl rings in biphenyl.[37−39] The in-plane ring−ring scissoring mode at 137 cm^{-1}, the out-of-plane ring−ring shearing mode at 267 cm^{-1}, and the in-plane ring−ring shearing mode at 312 cm^{-1} are

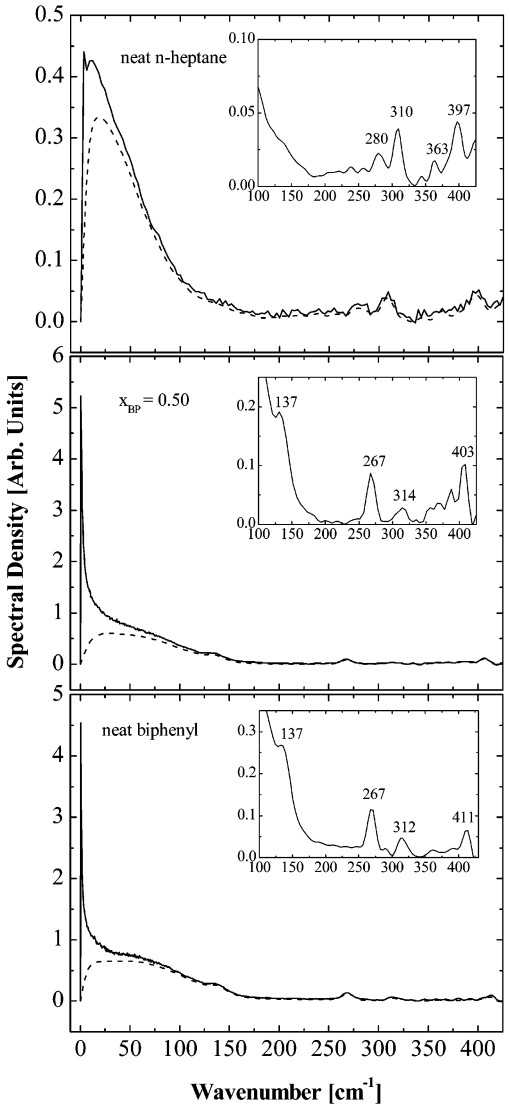

Figure 3. Spectral densities at 348 K for neat biphenyl, biphenyl/*n*-heptane mixture with $x_{BP} = 0.50$, and neat *n*-heptane. Solid curves are the full spectral densities; dashed curves are the reduced spectral densities.

evident in the spectrum of neat biphenyl shown in Figure 3. The band at 411 cm^{-1} is less certain and has been assigned either to a combination band involving an out-of-plane C−H bend and a C−C ring stretch[37] or to a combination band involving an out-of-plane C−H stretch and an in-plane ring−ring scissoring mode.[38] (The terms in-plane and out-of-plane strictly do not apply to the vibrations of biphenyl in the twisted state. However, the convention in the literature is to describe the vibrations of the twisted state in terms of the analogous vibrations of the planar state.) The torsional vibration about the central C−C bond has never been observed in the liquid phase. Calculations predict the frequency of the torsional vibration to be ∼60−70 cm^{-1}.[39] The RSD of biphenyl, however, does not show evidence for an intramolecular band at that frequency.

The intramolecular bands at 280, 310, 363, and 397 cm^{-1} in the spectral density of *n*-heptane have been observed previously in Raman scattering experiments.[40−42] The bands at 310, 363, and 397 cm^{-1} are the so-called acoustic modes associated with the accordion-like vibrations of the chain.[41] The band at 310 cm^{-1} is the longitudinal acoustic mode (LAM) associated with the vibration of the molecule in the all-trans conformation, while the other two bands correspond to the

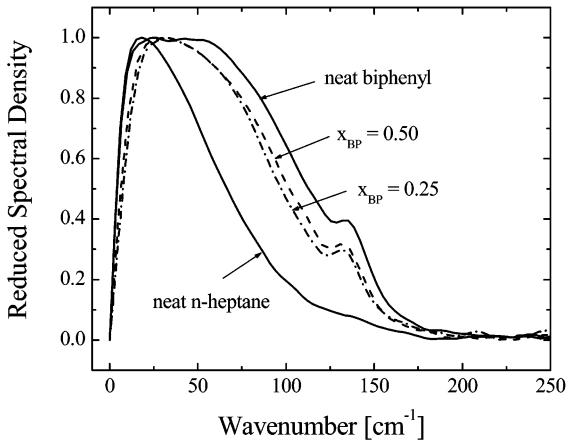

Figure 4. Comparison of reduced spectral densities at 348 K for neat n-biphenyl, biphenyl/*n*-heptane mixtures with $x_{BP} = 0.50$ and 0.25, and neat *n*-heptane.

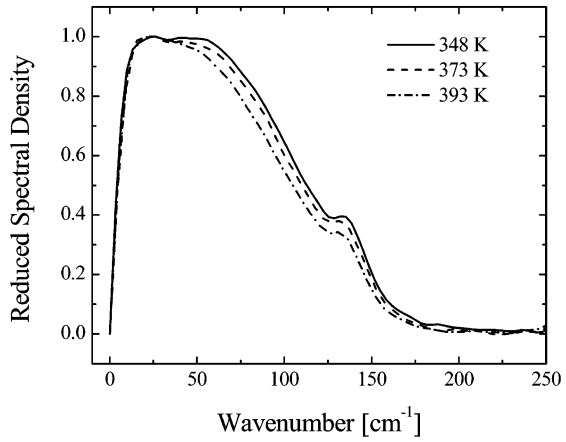

Figure 5. Reduced spectral density of neat biphenyl as a function of temperature.

vibrations of rotamers with straight-chain segments shorter than the all-trans conformation.[41]

Figure 4 compares the low-frequency RSDs of neat *n*-heptane, neat biphenyl, and biphenyl in *n*-heptane solution at 348 K. The RSD of *n*-heptane is a single asymmetric band with a well-defined peak at ≈18 cm^{-1} and a full width at half-maximum (fwhm) of ≈61 cm^{-1}. In contrast, the RSD of biphenyl is flat and considerably broader than that of *n*-heptane, with a fwhm of ≈106 cm^{-1}. The RSD of biphenyl is distinctly bimodal, as evidenced by the small dip at the top of the band, resembling the RSD of benzene at low temperatures.[2,43] In going from neat biphenyl to $x_{BP} = 0.25$, the RSD not only narrows but also dramatically changes in shape. For example, the dip in the middle is gone and the spectrum now falls off more rapidly on the low-frequency side than in the spectra of either neat biphenyl or neat *n*-heptane. Similar behavior is observed when benzene is diluted in CCl_4.[16] These changes indicate that the spectrum of the mixture cannot be simply regarded as a linear superposition of the spectra of the neat liquids but reflects the dynamics of biphenyl in solution.

Figure 5 shows the evolution of the RSD of neat biphenyl as the temperature is increased from 348 to 393 K. As can be seen in this figure, the bimodal structure is a strong function of temperature. With increasing temperature the intensity of the high-frequency shoulder decreases at a faster rate than the low-frequency shoulder. This change in the relative intensities of the two component bands results in a decrease in the fwhm of the overall band.

TABLE 4: Fit Parameters for the RSDs of Neat Biphenyl, Neat *n*-Heptane, and Biphenyl/*n*-Heptane Solution between 0 and 200 cm^{-1} [a,b]

liquid/mixture[c]	A_{BL}	a	ω_{BL}/cm^{-1}	A_{G1}	ω_{G1}/cm^{-1}	ϵ_{G2}/cm^{-1}	A_{G2}	ω_{G2}/cm^{-1}	ϵ_{G2}/cm^{-1}
neat BP at 393 K	0.114	1.12	11.4	0.96	48.2	49.11	0.123	135	9.50
	0.137	1.00	13.0	0.88	53.5	47.4	0.123	135	9.37
neat BP at 373 K	0.097	1.20	10.6	0.98	52.9	48.6	0.135	137	9.36
	0.132	1.00	13.2	0.89	59.4	46.2	0.136	137	9.36
neat BP at 348 K	0.129	1.08	10.9	1.07	48.8	51.8	0.134	138	8.25
	0.146	1.00	11.9	1.01	52.5	50.6	0.134	138	8.21
$x_{BP} = 0.50$ at 348 K	0.050	1.39	11.0	1.01	44.1	50.0	0.119	136	7.45
	0.098	1.00	17.6	0.72	62.3	43.9	0.121	137	7.65
$x_{BP} = 0.25$ at 348 K	0.020	1.75	9.36	1.17	35.7	49.3	0.130	136	9.29
	0.090	1.00	29.1	0.26	77.9	25.5	0.140	134	9.87
neat C_7 at 348 K	0.22	0.74	28.7						
	0.12	1.00	23.7						

[a] See eqs 7 and 8 for definition of parameters. [b] For the component bands of a given liquid/mixture, the first set of parameters correspond to the BLAG model and the second set of parameters correspond to the OAG model (see text). [c] BP, biphenyl; C_7, *n*-heptane.

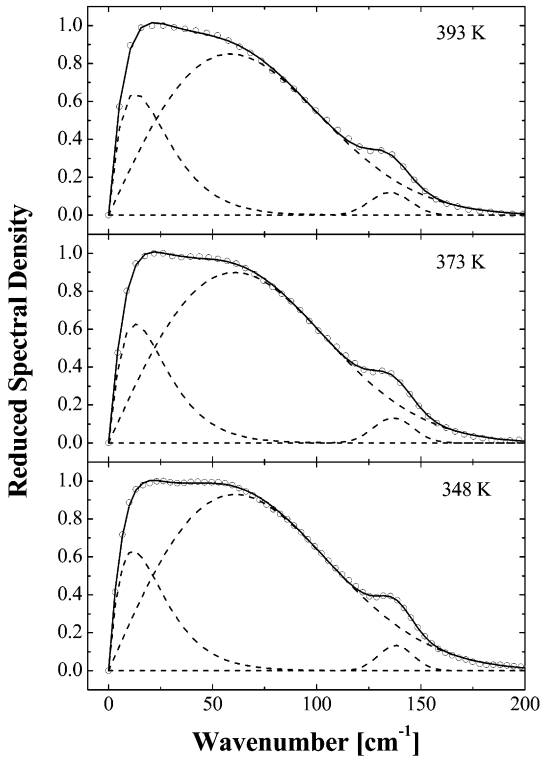

Figure 6. Reduced spectral densities in the region 0−200 cm^{-1} for neat biphenyl as a function of temperature (open circles) with BLAG model fits (solid lines). The low-frequency component is given by the Bucaro−Litovitz function (eq 7) with exponent *a* freely varying in the fit, and the high-frequency component is given by the antisymmetrized Gaussian function (eq 8). The intramolecular band at 137 cm^{-1} is fit by an antisymmetrized Gaussian function. See Table 4 for the fit parameters.

On the basis of kinematics alone (i.e., moments of inertia), it is not surprising that the RSD of biphenyl is bimodal. In principle, there should be two rotational contributions to the RSD: a high-frequency contribution associated with the smaller moment of inertia and a low-frequency contribution associated with the two larger moments of inertia. On the basis of the MD simulations of Ryu and Stratt,[8] we expect that translations should give rise to another contribution to the RSD that is lower in frequency than the rotational contributions. The RSD of biphenyl, however, does not appear to exhibit additional structure that would indicate the presence of three different types of motion. If a translational contribution is present, it must be overlapped with the low-frequency rotational contribution. There is, however, no a priori way of determining to what extent these motions contribute to the low-frequency component of the RSD.

Bimodal Line Shape Analysis. To quantify the observed spectral changes, the RSDs were fit to a bimodal line shape function

$$I(\omega) = I_{BL}(\omega) + I_G(\omega) \tag{6}$$

where the low-frequency component is the Bucaro−Litovitz function,

$$I_{BL}(\omega) = A_{BL}\omega^a \exp(-\omega/\omega_{BL}) \tag{7}$$

and the high-frequency component is the antisymmetrized Gaussian function

$$I_G(\omega) = A_G\{\exp[-(\omega - \omega_G)^2/2\epsilon^2] - \exp[-(\omega + \omega_G)^2/2\epsilon^2]\} \tag{8}$$

The Bucaro−Litovitz function was first introduced to account for the collision-induced part of the light-scattering spectrum of spherical or nearly spherical polarizable molecular liquids.[44] The Bucaro−Litovitz function with $a = 1$ is known as the Ohmic function. The antisymmetrized form of the Gaussian, which is used to represent the part of the intermolecular spectrum associated with rotational motion, satisfies the requirement that the RSD goes to zero at $\omega = 0$. We will refer to the bimodal line shape function with exponent *a* freely varying in the fits as the BLAG model and with exponent *a* set equal to 1 in the fits as the OAG model. Although these phenomenological models have been applied to the analysis of spectra of polar and nonpolar molecular liquids[11,13,14,45,46] and complex fluids, such as liquid crystals[29] and ionic liquids,[28] their use cannot always be physically justified.[2] Indeed, Ryu and Stratt[8] showed that coupling of the rotational motion of a benzene molecule to the collective translational motion of the first shell of nearest neighbors causes the rotational component to extend to lower frequency.

Figures 6−9 show the results of this bimodal analysis, where the intermolecular band is fit by either the BLAG model or the OAG model and the intramolecular band at 137 cm^{-1} is fit by an antisymmetrized Gaussian function. Note that the RSD of neat *n*-heptane can be well fit only by using the Bucaro−Litovitz function. Clearly, a poorer fit is obtained for neat *n*-heptane using the Ohmic function, where only two parameters are allowed to vary instead of all three. The corresponding fit parameters for the fits in Figures 6−9 are given in Table 4.

TABLE 5: Spectral Parameters for the Intermolecular Spectra of Neat Biphenyl, Neat *n*-Heptane, and Biphenyl/*n*-Heptane Mixtures between 0 and 200 cm^{-1} [a,b]

	intermolecular spectrum[d]		low-frequency component			high-frequency component		
liquid/mixture[c]	$\langle\omega\rangle$[e]/cm^{-1}	fwhm[f]/cm^{-1}	ω_{max}[g]/cm^{-1}	fwhm[f]/cm^{-1}	area[h]	ω_{max}[g]/cm^{-1}	fwhm[f]/cm^{-1}	area[h]
neat BP at 393 K	61.8	99.6	10.5	31.5	0.206	57.7	94.3	0.794
			15.7	31.4	0.228	57.7	94.3	0.772
neat BP at 373 K	63.8	101.8	13.1	30.7	0.185	61.3	92.0	0.815
			13.1	35.1	0.217	61.3	96.4	0.783
neat BP at 348 K	65.3	105.6	13.2	29.7	0.175	59.4	95.7	0.825
			13.2	29.7	0.185	62.7	95.7	0.815
$x_{BP} = 0.50$ at 348 K	62.2	94.3	15.7	31.5	0.193	57.7	89.1	0.807
			15.7	47.2	0.311	62.9	89.1	0.689
$x_{BP} = 0.25$ at 348 K	60.3	91.9	16.0	28.0	0.153	56.0	84.0	0.847
			28.0	72.0	0.823	80.0	55.0	0.177
neat C_7 at 348 K	48.4	60.6	18.2	60.6				

[a] Errors in $\langle\omega\rangle$, ω_{max}, and fwhm are ± 1 cm^{-1}; error in area is $\pm 2\%$. [b] For the component bands of a given liquid/mixture, the first set of parameters correspond to the BLAG model and the second set of parameters correspond to the OAG model (see text). [c] BP, biphenyl; C_7, *n*-heptane. [d] Spectral parameters for the intermolecular part of RSD. [e] First spectral moment. [f] Full width at half-maximum. [g] Frequency at the peak of the band. [h] Area under the band (arbitrary units).

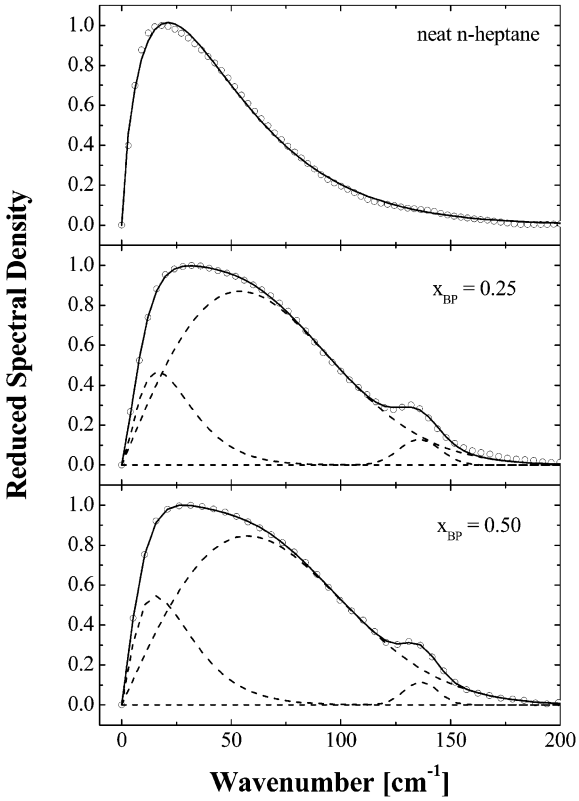

Figure 7. Reduced spectral densities for neat *n*-heptane and biphenyl/*n*-heptane mixtures at 348 K (open circles) with BLAG model fits (solid lines). The low-frequency component is given by the Bucaro−Litovitz function (eq 7) with exponent *a* freely varying in the fit, and the high-frequency component is given by the antisymmetrized Gaussian function (eq 8). The intramolecular band at 137 cm^{-1} in the RSD of biphenyl/*n*-heptane mixtures was fit by an antisymmetrized Gaussian function. See Table 4 for the fit parameters.

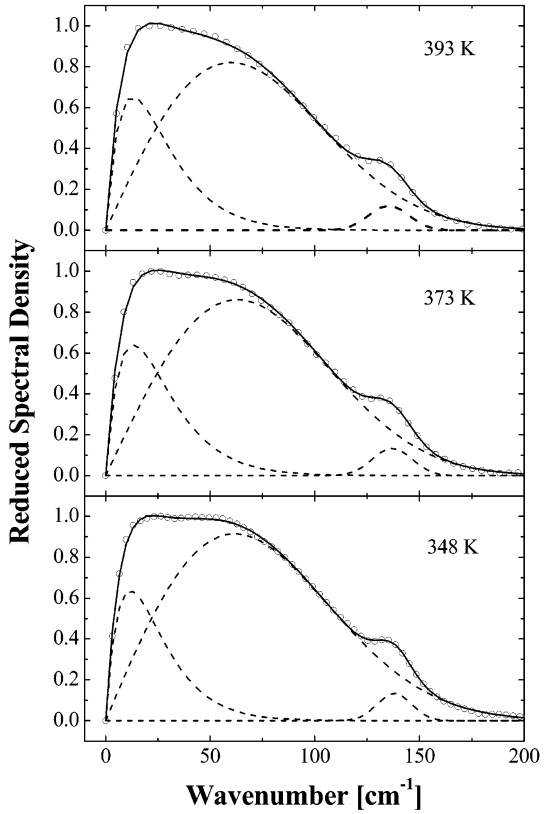

Figure 8. Reduced spectral densities in the region 0−200 cm^{-1} for neat biphenyl as a function of temperature (open circles) with OAG model fits (solid lines). The low-frequency component is given by the Bucaro−Litovitz (eq 7) with exponent *a* set equal to 1 (Ohmic function), and the high-frequency component is given by the antisymmetrized Gaussian function (eq 8). The intramolecular band at 137 cm^{-1} is fit by an antisymmetrized Gaussian function. See Table 4 for the fit parameters.

Not surprisingly, the fit parameters for the intramolecular band are essentially independent of the model used to fit the intermolecular band.

Fitting the RSDs in this way allows us to separate the intermolecular and intramolecular contributions in the RSD and to examine the effects of temperature and dilution on the intermolecular part of the RSD. Table 5 lists the values of the first spectral moment, $\langle\omega\rangle$, and the fwhm for the intermolecular band, and the peak frequency, ω_{max}, and fwhm for the component bands, as well as the relative contributions of the component bands to the overall intermolecular band. The first spectral moment is a useful parameter for characterizing the RSDs when the band is flat or when there is no well-defined peak, as in biphenyl.

As the temperature is increased from 348 to 393 K, the value of $\langle\omega\rangle$ decreases from 65.3 to 61.8 cm^{-1} while the fwhm decreases from 105.6 to 99.6 cm^{-1}. This behavior is consistent with behavior observed in other systems.[2,13,43,47−49] Within the context of the quantum HO model, these spectral changes can be related to the decrease in the frequency of the oscillator. Since the density of the liquid decreases as the temperature is

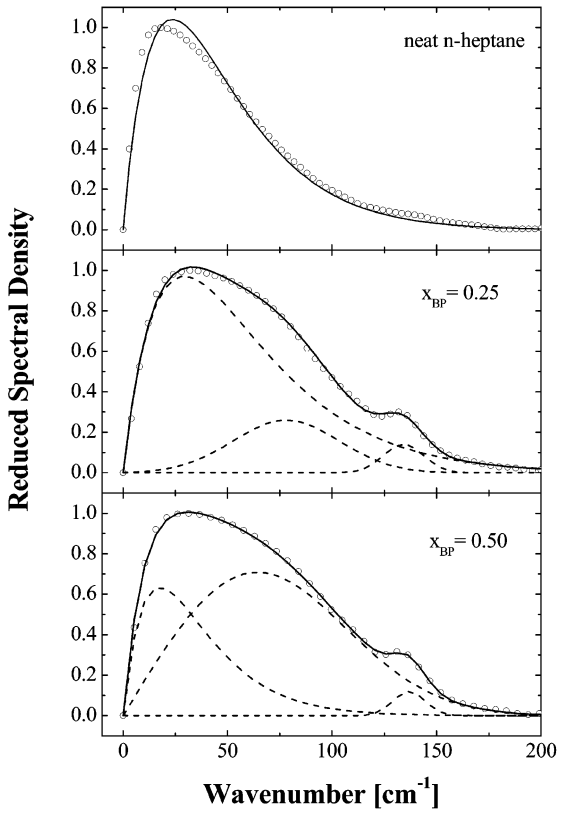

Figure 9. Reduced spectral densities for neat *n*-heptane and biphenyl/*n*-heptane mixtures at 348 K (open circles) with OAG model fits (solid lines). The low-frequency component is given by the Bucaro−Litovitz function (eq 7) with exponent *a* set equal to 1 (Ohmic function), and the high-frequency component is given by the antisymmetrized Gaussian function (eq 8). The intramolecular band at 137 cm^{-1} in the RSD of biphenyl/*n*-heptane mixtures was fit by an antisymmetrized Gaussian function. See Table 4 for the fit parameters.

increased, one expects the intermolecular potential to become less steep and therefore the frequencies of the intermolecular modes to decrease.[50]

The effect of dilution on the intermolecular band is also consistent with behavior observed previously in other systems.[13,33,35,36,51] In going from the neat liquid at 348 K to $x_{BP} = 0.25$ at 348 K, the value of $\langle\omega\rangle$ decreases from 65.3 to 60.3 cm^{-1} and fwhm decreases from 105.6 to 91.9 cm^{-1}. Again, the quantum HO model provides insight into these spectral changes. The shift toward lower frequency and narrowing of the RSD of biphenyl in *n*-heptane can be attributed to a decrease in the curvature of the intermolecular potential associated with the oscillator. This decrease can be understood in terms of the relative magnitudes of the biphenyl−biphenyl and biphenyl−*n*-heptane interactions. Because the polarizability of biphenyl is much larger than that of *n*-heptane (Table 1),[23,52] biphenyl−biphenyl interactions will be stronger than biphenyl−*n*-heptane interactions. Therefore, as biphenyl molecules are successively replaced by *n*-heptane molecules, one expects the frequencies of the intermolecular modes to decrease.[9,33−35]

If the bimodal character of the intermolecular band is due to collective modes associated with specific motions in the liquid, the individual component bands in the models should behave in the same way as the overall intermolecular band. This, however, is not the case. We first note that the parameters of the component bands in the OAG model are different than those in BLAG model. This difference in the values of the fit parameters for the two models can be attributed to the fact that the parameters in the Bucaro−Litovitz function are strongly correlated to each other. Best fits of the BLAG model are obtained for $a > 1$ (see Table 4). For these fits, A_{BL} and ω_{BL} tend to be lower than the corresponding values for $a = 1$ in the OAG model. The larger the deviation of the exponent *a* from unity, the greater the fit parameters in the BLAG model differ from the corresponding values in the OAG model. This can lead to the component bands behaving differently in the two models.

Comparing the fits in Figures 6 and 8 and the spectral parameters in Table 5, the effect of temperature on the component bands in the OAG model is different from that in the BLAG model. For the low-frequency component in the BLAG model, the value of ω_{max} decreases from 13.2 to 10.5 cm^{-1} while its fwhm exhibits a slight increase from 29.7 to 31.5 cm^{-1} as the temperature is increased from 348 to 393 K. In the OAG model, the value of ω_{max} for the low-frequency component increases, from 13.2 to 15.7 cm^{-1}, while its fwhm remains at the constant value of 32.1 ± 2.7 cm^{-1} as the temperature is increased from 348 to 393 K. However, for both models, the frequency and width of the high-frequency component are independent of temperature, with $\omega_{max} = 60.0 \pm 2.0$ cm^{-1} and fwhm = 94.7 ± 1.6 cm^{-1}.

Comparing the fits in Figures 7 and 9 and the spectral parameters in Table 5, the effect of dilution on the component bands in the OAG model is strikingly different from that in the BLAG model. In the BLAG model, the value of ω_{max} for the low-frequency component increases only from 13.2 to 16.0 cm^{-1} while its fwhm remains at the constant value of 30.0 ± 1.4 cm^{-1} in going from neat biphenyl to $x_{BP} = 0.25$. However, in the OAG model, the increase in the corresponding parameters for the low-frequency component is much larger, from $\omega_{max} =$ 13.2 cm^{-1} and fwhm = 29.7 cm^{-1} for neat biphenyl to $\omega_{max} =$ 28.0 cm^{-1} and fwhm = 72.0 cm^{-1} at $x_{BP} = 0.25$. Similarly, in the case of the high-frequency component, the value of ω_{max} in the BLAG model decreases slightly from 59.4 to 56.0 cm^{-1} while its fwhm decreases from 95.7 to 84 cm^{-1} in going from neat biphenyl to $x_{BP} = 0.25$. On the other hand, for the high-frequency component in the OAG model, the value of ω_{max} remains at the constant value of ≈63 cm^{-1} in going from neat biphenyl to $x_{BP} = 0.50$, and then increases to 80.0 cm^{-1} at $x_{BP} = 0.25$, while its fwhm decreases continuously from 95.7 cm^{-1} in neat biphenyl to 55.0 cm^{-1} at $x_{BP} = 0.25$.

With respect to the frequencies and widths of the component bands, neither model gives behavior that is physically consistent. The only aspect of these models that makes physical sense is the relative contribution of the component bands to the intermolecular band. As the temperature is increased from 348 to 393 K, the contribution of the high-frequency component to the intermolecular band decreases, from 82.5% to 79.4% in the BLAG model and from 81.5% to 77.2% in the OAG model. This decrease contributes to the shift of the intermolecular band toward lower frequencies that occurs as the density of the liquid decreases. One also expects the contribution of the high-frequency component to decrease with increasing dilution as the biphenyl−biphenyl interactions are replaced with biphenyl−*n*-heptane interactions. In this regard, the OAG model is physically more sensible than the BLAG model. In going from neat biphenyl to $x_{BP} = 0.25$, the contribution of the high-frequency component decreases from 81.5% to 17.7% in the OAG model, but remains at the constant value of 83% ± 2% in the BLAG model.

Liquid Structure and Intermolecular Dynamics. Figure 10 compares the RSD of biphenyl at 373 K with the RSD of benzene at 293 K, which was obtained in a previous study.[14]

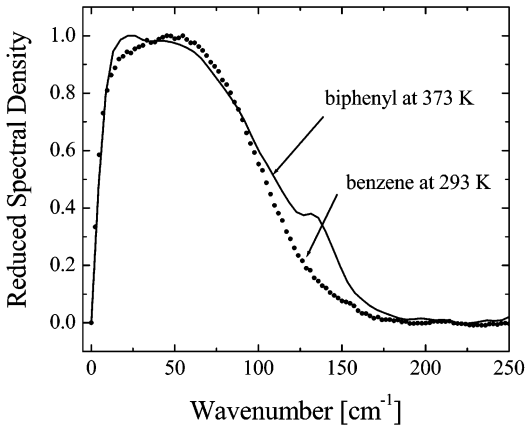

Figure 10. Comparison of reduced spectral densities for neat biphenyl at 373 K and neat benzene at 293 K.

The mean frequency and width are slightly larger for biphenyl than for benzene. The first spectral moment and fwhm are, respectively, 54.8 and 100 cm^{-1} for liquid benzene at 293 K versus 63.8 and 101.8 cm^{-1} for liquid biphenyl at 373 K. Also, the low-frequency shoulder is more pronounced in biphenyl than in benzene. Despite these differences and the difference in temperature, it is remarkable how well the two RSDs overlap each other, considering that the moments of inertia are larger for biphenyl than for benzene (Table 2). Within the context of the quantum HO model, we attribute the similarity of the RSDs to the force constant of the oscillator being larger in liquid biphenyl than in liquid benzene.

To quantify this difference in force constants, we will assume that the RSDs are largely determined by rotational dynamics. In light of the MD simulations of Ryu and Stratt,[8] this assumption is justified for benzene. On the basis of the line shape analysis above, the largest contribution to the RSD of biphenyl comes from the high-frequency component. Therefore this assumption is also physically reasonable for biphenyl. If the rotational frequency is given by $(k/I)^{1/2}$, where k is the force constant and I is the moment of inertia, the ratio of the force constants is given by

$$\frac{k_{\text{biphenyl}}}{k_{\text{benzene}}} = \left[\frac{\omega_{\text{biphenyl}}}{\omega_{\text{benzene}}}\right]^2 \frac{I_{\text{biphenyl}}}{I_{\text{benzene}}} \tag{9}$$

To calculate this ratio, the rotational frequency is taken to be equal to $\langle\omega\rangle$. The rotational dynamics in benzene are due to the tumbling motion of the molecule. We will assume, given the relative magnitudes of the moments of inertia, that the rotational dynamics in biphenyl are primarily due to the spinning motion of the molecule. Substituting the moment of inertia I_B for benzene, which is associated with rotation about the 2-fold axis, the moment of inertia I_A for biphenyl, which is associated with rotation about the long axis, and the frequencies $\langle\omega\rangle_{\text{biphenyl}} \approx 64$ cm^{-1} and $\langle\omega\rangle_{\text{benzene}} \approx 55$ cm^{-1} into eq 9, we find that the force constant ratio is equal to ≈2.7. This analysis is obviously very simplistic because the intermolecular part of the RSD cannot be ascribed to a single mode but is a weighted distribution of frequencies corresponding to the intermolecular modes of the liquid. Despite its simplicity, this heuristic approach, which has been used previously,[13,14] gives us a way of understanding the RSDs of liquids in terms of quantities that are characteristic of the intermolecular forces, such as a force constant or the curvature of the intermolecular potential.

What could cause this difference in force constants? On the basis of the densities of the liquids and the molecular volumes, one would not expect the intermolecular potential to be steeper in liquid biphenyl than in liquid benzene. At 348 K and 1 atm, the density of liquid biphenyl is 0.9914 g/mL.[53] At this density, the average volume per molecule is ≈258 Å^3, whereas the van der Waals volume of biphenyl is 150 Å^3.[54] At 293 K and 1 atm, the density of benzene is 0.8765 g/mL.[53] At this density, the average volume per molecule is ≈147 Å^3, whereas the van der Waals volume of benzene is 80 Å^3.[54] Thus, the percentage of the volume per molecule in the liquid due to the molecular volume is 58% for biphenyl and 54% for benzene. This percentage is roughly the same for biphenyl and benzene, because the volume of a biphenyl molecule is roughly equal to the volume of two benzene molecules. The above calculations do not, however, take into account molecular shape or packing effects.

The diffusive orientational dynamics suggest that biphenyl molecules behave like cylindrical ellipsoids. If we consider free rotation, then the spinning motion should be ∼5−6 times faster than the tumbling motion, based on the moments of inertia. It is therefore reasonable to assume that biphenyl molecules will pack like cylindrical ellipsoids, with molecules locally aligned parallel to each other. (Consider the average arrangement of neighboring Tootsie Rolls in a candy jar.) Let us assume that the radius of the ellipsoid is equal to half the width of a phenyl ring and the length of the ellipsoid is equal to the distance between the hydrogen atoms at the ends of the long axis. From space-filling models, we estimate the radius and the length of the ellipsoid to be, respectively, 3.2 and 11.3 Å. The cylindrical volume that the molecule sweeps out as it rotates about its long axis would therefore be equal to 352 Å^3. This volume is 36% larger than the average volume per molecule in the liquid. If we assume that a benzene molecule undergoes tumbling motion, then it effectively sweeps out a spherical volume equal to ∼180 Å^3, which is only 18% larger than the volume per molecule in the liquid. (Our estimates of molecular dimensions take into account the van der Waals radii of the hydrogen atoms (≈1 Å).[55]) These calculations indicate that molecular packing restricts the rotational motion to a larger extent in liquid biphenyl than in liquid benzene, which is consistent with the curvature of the intermolecular potential being larger in liquid biphenyl than in liquid benzene. Moreover, one could argue that because the molecules are locally aligned parallel to each other, the range of angular motion will be smaller for tumbling than for spinning in liquid biphenyl. Indeed, if we attribute the RSD of biphenyl to the tumbling motion of the molecules, we obtain a much larger force constant ratio of ∼14. The high-frequency component of the RSD could therefore also have a contribution arising from the tumbling motion of the molecules. Unfortunately, the relative contributions from each of these motions cannot be determined from the OHD-OKE data.

V. Conclusions

The RSD of liquid biphenyl is broad and structured. As Ryu and Stratt[8] showed for benzene, one can rationalize the structure of the RSD of biphenyl in terms of the moments of inertia. For biphenyl, the two moments of inertia associated with tumbling motion about the short axes are considerably larger than the moment of inertia associated with spinning motion about the long axis. Because of these distinct moments of inertia, the rotational contribution to the RSD of biphenyl is broad. The spectrum of biphenyl undergoes a red shift and line narrowing with temperature and upon dilution in *n*-heptane. These effects are also accompanied by changes in the spectral features that characterize the RSD. For example, upon dilution the dip in

the middle that is a signature of its bimodal structure disappears and the spectrum falls off more rapidly on the low-frequency side than in the spectra of either neat biphenyl or neat *n*-heptane. In addition, the intensity of the high-frequency shoulder decreases at a faster rate than the low-frequency shoulder with temperature. The RSD of biphenyl can be well fit by a bimodal line shape function composed of a low-frequency component and a high-frequency component. However, inconsistencies arise in the interpretation of the effects of temperature and dilution on the individual component bands. These inconsistencies expose the shortcomings in using phenomenological models to assign features in an RSD to specific molecular motions. Packing models suggest that rotational motion is more hindered in liquid biphenyl than in liquid benzene. This could explain why the RSD of biphenyl is similar to that of benzene in frequency and width, even though the moments of inertia for biphenyl are larger than the moments of inertia for benzene. Clearly, further work is needed to understand the similarities between benzene and biphenyl.

Acknowledgment. We gratefully acknowledge the support of this research by the Welch Foundation. We thank the reviewers for their helpful comments.

References and Notes

(1) Kinoshita, S.; Kai, Y.; Ariyoshi, T.; Shimada, Y. *Int. J. Mod. Phys. B* **1996**, 10.
(2) Fourkas, J. T. In *Ultrafast Infrared and Raman Spectroscopy*; Fayer, M. D., Ed.; Marcel Dekker: New York, 2001.
(3) Smith, N.; Meech, S. R. *Int. Rev. Phys. Chem.* **2002**, *21*, 75.
(4) Murry, R. L.; Fourkas, J. T.; Keyes, T. *J. Chem. Phys.* **1998**, *109*, 2814.
(5) Ji, X.; Ahlborn, H.; Space, B.; Moore, P. B. *J. Chem. Phys.* **2000**, *113*, 8693.
(6) Torii, H.; Tasumi, M. *J. Phys. Chem. A* **2000**, *104*, 4174.
(7) Skaf, M. S.; Vechi, S. M. *J. Chem. Phys.* **2003**, *119*, 2181.
(8) Ryu, S.; Stratt, R. M. *J. Phys. Chem. B* **2004**, *108*, 6782.
(9) McMorrow, D.; Thantu, N.; Kleinman, V.; Melinger, J. S.; Lotshaw, W. T. *J. Phys. Chem. A* **2001**, *105*, 7960.
(10) McMorrow, D.; Lotshaw, W. T. *Chem. Phys. Lett.* **1993**, *201*, 369.
(11) Chang, Y. J.; Castner, E. W. J. *J. Phys. Chem.* **1996**, *100*, 3330.
(12) Cong, P.; Deuel, H. P.; Simon, J. D. *Chem. Phys. Lett.* **1995**, *240*, 72.
(13) Smith, N.; Meech, S. R. *J. Phys. Chem. A* **2000**, *104*, 4223.
(14) Neelakandan, M.; Pant, D.; Quitevis, E. L. *J. Phys. Chem. A* **1997**, *101*, 2936.
(15) Smith, N. A.; Lin, S.; Meech, S. R.; Yoshihara, K. *J. Phys. Chem. A* **1997**, *101*, 3641.
(16) Lotshaw, W. T.; Staver, P. R.; McMorrow, D.; Thantu, N.; Melinger, J. S. *Springer Ser. Chem. Phys.* **1994**, *60*, 91.
(17) Chelli, R.; Cardini, G.; Procacci, P.; Righini, R.; Califano, S.; Albrecht, A. *J. Chem. Phys.* **2000**, *113*, 6851.
(18) Chelli, R.; Cardini, G.; Ricci, M.; Bartolini, P.; Righini, R.; Califano, S. *Phys. Chem. Chem. Phys.* **2001**, *3*, 2803.
(19) Ratajska-Gadomska, B.; Gadomski, W.; Wiewior, P.; Radzewicz, C. *J. Chem. Phys.* **1998**, *108*, 8489.
(20) Ratajska-Gadomska, B. *J. Chem. Phys.* **2002**, *116*, 4563.
(21) Lowden, L. J.; Chandler, D. *J. Chem. Phys.* **1974**, *61*, 5228.
(22) Chandler, D. *Annu. Rev. Phys. Chem.* **1978**, *29*, 441.
(23) McKenney, J. D.; Gottschalk, K. E.; Pedersen, L. *J. Mol. Struct.* **1983**, *105*, 427.
(24) Suzuki, H. *Bull. Chem. Soc. Jpn.* **1959**, *32*, 1340.
(25) Eaton, V. J.; Steele, D. *J. Chem. Soc., Faraday Trans. 2* **1973**, *69*, 1601.
(26) Deeg, F. W.; Stankus, J. J.; Greenfield, S. R.; Newell, V. J.; Fayer, M. D. *J. Chem. Phys.* **1989**, *90*, 6893.
(27) Nikomanis, F.; Samios, D.; Dorfmuller, T. *J. Mol. Liq.* **1989**, *43*, 271.
(28) Hyun, B. R.; Dzyuba, S. V.; Bartsch, R. A.; Quitevis, E. L. *J. Phys. Chem. A* **2002**, *106*, 7579.
(29) Hyun, B. R.; Quitevis, E. L. *Chem. Phys. Lett.* **2003**, *370*, 725.
(30) McMorrow, D.; Lotshaw, W. T. *J. Phys. Chem.* **1991**, *95*, 10395.
(31) McMorrow, D. *Opt. Commun.* **1991**, *86*, 236.
(32) Kinoshita, S.; Kai, Y.; Yamaguchi, M.; Yagi, T. *Phys. Rev. Lett.* **1995**, *75*, 148.
(33) Kalpouzos, C.; McMorrow, D.; Lotshaw, W. T.; Kenney-Wallace, G. A. *Chem. Phys. Lett.* **1988**, *150*, 138.
(34) Kalpouzos, C.; McMorrow, D.; Lotshaw, W. T.; Kenney-Wallace, G. A. *Chem. Phys. Lett.* **1989**, *155*, 240.
(35) McMorrow, D.; Thantu, N.; Melinger, J. S.; Kim, S. K.; Lotshaw, W. T. *J. Phys. Chem.* **1996**, *100*, 10389.
(36) Steffen, T.; Meinders, N. A. C. M.; Duppen, K. *J. Phys. Chem. A* **1998**, *102*, 4213.
(37) Katon, J. E.; Lippincott, E. R. *Spectrochim. Acta* **1959**, 627.
(38) Steele, D.; Lippincott, E. R. *J. Mol. Spectrosc.* **1961**, *6*, 238.
(39) Barrett, R. M.; Steele, D. *J. Mol. Struct.* **1972**, *11*, 105.
(40) Mizushima, S.-I.; Simanouti, T. *J. Am. Chem. Soc.* **1949**, *71*, 1320.
(41) Schaufele, R. F. *J. Chem. Phys.* **1968**, *49*, 4168.
(42) Schoen, P. E.; Priest, R. G.; Sheridan, J. P.; Schnur, J. M. *J. Chem. Phys.* **1979**, *71*, 317.
(43) Ricci, M.; Bartolini, P.; Chelli, R.; Cardini, G.; Califano, S.; Righini, R. *Phys. Chem. Chem. Phys.* **2001**, *3*, 2795.
(44) Bucaro, J. A.; Litovitz, T. A. *J. Chem. Phys.* **1970**, *54*, 3846.
(45) Chang, Y. J.; Castner, E. W. J. *J. Chem. Phys.* **1993**, *99*, 7289.
(46) Chang, Y. J.; Castner, E. W. J. *J. Phys. Chem.* **1994**, *98*, 9712.
(47) Farrer, R. A.; Loughnane, B. J.; Deschenes, L. A.; Fourkas, J. T. *J. Chem. Phys.* **1997**, *106*, 6901.
(48) Lotshaw, W. T.; McMorrow, D.; Thantu, N.; Melinger, J. S.; Kitchenham, R. *J. Raman Spectrosc.* **1995**, *26*, 571.
(49) Bartolini, P.; Ricci, M.; Torre, R.; Righini, R. *J. Chem. Phys.* **1999**, *110*, 8653.
(50) Ruhman, S.; Kohler, B.; Joly, A. G.; Nelson, K. A. *Chem. Phys. Lett.* **1987**, *141*, 16.
(51) Hyun, B. R.; Quitevis, E. L. *Chem. Phys. Lett.* **2003**, *373*, 526.
(52) Bhaumik, D.; Jaffe, H. H.; Mark, J. E. *J. Mol. Struct.* **1982**, *87*, 81.
(53) *Lange's Handbook of Chemistry*; Dean, J. A., Ed.; McGraw-Hill: New York, 1985.
(54) Berne, B.; Pecora, R. *Dynamic Light Scattering*, 1st ed.; Wiley: New York, 1976.
(55) Bondi, A. *J. Phys. Chem.* **1964**, *68*, 441.